THE JOURNAL OF BIOLOGICAL CHEMISTRY VOL. 281, NO. 43, pp. 32619–32629, October 27, 2006

Proteomic Identification of Novel Substrates of a Protein Isoaspartyl Methyltransferase Repair Enzyme*[S]

Received for publication, June 6, 2006, and in revised form, August 17, 2006 Published, JBC Papers in Press, August 21, 2006, DOI 10.1074/jbc.M605421200

Vasanthy Vigneswara[‡], Jonathan D. Lowenson[§], Claire D. Powell[‡], Matthew Thakur[‡], Kevin Bailey[‡], Steven Clarke[§], David E. Ray[‡], and Wayne G. Carter[‡1]

From the [‡]Medical Research Council Applied Neuroscience Group, School of Biomedical Sciences, The University of Nottingham, Queen's Medical Centre, Nottingham NG7 2UH, United Kingdom and the [§]Department of Chemistry and Biochemistry, University of California, Los Angeles, California 90095

We report the use of a proteomic strategy to identify hitherto unknown substrates for mammalian protein L-isoaspartate *O*-methyltransferase. This methyltransferase initiates the repair of isoaspartyl residues in aged or stress-damaged proteins *in vivo*. Tissues from mice lacking the methyltransferase (*Pcmt1*$^{-/-}$) accumulate more isoaspartyl residues than their wild-type littermates, with the most "damaged" residues arising in the brain. To identify the proteins containing these residues, brain homogenates from *Pcmt1*$^{-/-}$ mice were methylated by exogenous repair enzyme and the radiolabeled methyl donor *S*-adenosyl-[*methyl*-^{3}H]methionine. Methylated proteins in the homogenates were resolved by both one-dimensional and two-dimensional electrophoresis, and methyltransferase substrates were identified by their increased radiolabeling when isolated from *Pcmt1*$^{-/-}$ animals compared with *Pcmt1*$^{+/+}$ littermates. Mass spectrometric analyses of these isolated brain proteins reveal for the first time that microtubule-associated protein-2, calreticulin, clathrin light chains a and b, ubiquitin carboxyl-terminal hydrolase L1, phosphatidylethanolamine-binding protein, stathmin, β-synuclein, and α-synuclein, are all substrates for the L-isoaspartate methyltransferase *in vivo*. Our methodology for methyltransferase substrate identification was further supplemented by demonstrating that one of these methyltransferase targets, microtubule-associated protein-2, could be radiolabeled within *Pcmt1*$^{-/-}$ brain extracts using radioactive methyl donor and exogenous methyltransferase enzyme and then specifically immunoprecipitated with microtubule-associated protein-2 antibodies to recover co-localized protein with radioactivity. We comment on the functional significance of accumulation of relatively high levels of isoaspartate within these methyltransferase targets in the context of the histological and phenotypical changes associated with the methyltransferase knock-out mice.

There is a general decline in physiological processes with aging but the molecular changes that induce senescence or age-related pathologies have yet to be completely defined. It is thought, however, that the slow accumulation of damaged macromolecules as an organism ages probably contributes to the aging phenotype. Proteins, for example, are susceptible to undesired internal and external chemical modifications, including oxidation, glycation, deamidation, and isomerization, all of which can result in an alteration of protein function and/or stability (1, 2).

Cells have several strategies for removing damaged proteins, including lysosomal- and proteasomal-dependent degradation. Additionally, protein repair mechanisms exist to restore protein function without the requirement for *de novo* synthesis. One such protein repair enzyme, termed protein L-isoaspartate (D-aspartate) *O*-methyltransferase, PIMT[2] (EC 2.1.1.77, also known as protein carboxylmethyltransferase 1 (PCMT1)), initiates the repair of isoaspartate within peptide chains.

Isoaspartyl residues within peptides and proteins arise spontaneously by either deamidation of asparagine or isomerization of aspartic acid residues. Both reactions involve the formation of an intermediary five-membered L-succinimidyl ring, which is readily hydrolyzed to yield a normal L-aspartyl residue or an atypical L-isoaspartyl residue in which the peptide backbone now contains an extra methylene group and proceeds through the β-carboxyl group. The asymmetric nature of the succinimide ring favors hydrolysis resulting in an aspartate:isoaspartate ratio of ~1:3 (see Fig. 1). The rate of isoaspartate formation in proteins depends greatly on both amino acid sequence and conformation but is overall one of the most common forms of protein damage and reflects aging at the molecular level (2–4).

Methylation of isoaspartate by PIMT significantly increases the rate at which these damaged residues return to the succin-

* This work was supported by a UK Medical Research Council program grant (to D. E. R.) and by National Institutes of Health Grant GM026020 (to S. C. and J. D. L.). Purchase of a Multichannel Plate Detector was funded by the UK Dept. of the Environment, Food, and Rural Affairs. The costs of publication of this article were defrayed in part by the payment of page charges. This article must therefore be hereby marked "*advertisement*" in accordance with 18 U.S.C. Section 1734 solely to indicate this fact.

[S] The on-line version of this article (available at http://www.jbc.org) contains supplemental Tables S1 and S2.

[1] To whom correspondence should be addressed. Tel.: 44-(0)115-823-0176; Fax: 44-(0)115-823-0142; E-mail: wayne.carter@nottingham.ac.uk.

[2] The abbreviations used are: PIMT, protein L-isoaspartate *O*-methyltransferase; CAPS, 3-(cyclohexylamino)propane-1-sulfonic acid; IPG, immobilized pH gradient; MAPK, mitogen-activated protein kinase; MES, 2(*N*-morpholino)ethanesulfonic acid; K-MES, potassium-MES; PVDF, polyvinylidene difluoride; MALDI-TOF, matrix-assisted laser desorption ionization-time of flight; LC MS/MS, liquid chromatography and tandem mass spectrometry; MAP-2, microtubule-associated protein-2; AdoMet, *S*-adenosylmethionine; 1D, one-dimensional; 2D, two-dimensional; Bis-Tris, 2-[bis(2-hydroxyethyl)amino]-2-(hydroxymethyl)propane-1,3-diol; DTT, dithiothreitol; KO, knockout; CHAPS, 3-[(3-cholamidopropyl)dimethylammonio]-1-propanesulfonic acid; IP, immunoprecipitation; UCHL1, ubiquitin carboxyl-terminal hydrolase L1; PEBP, phosphatidylethanolamine-binding protein; GABA, γ-aminobutyric acid; ER, endoplasmic reticulum.

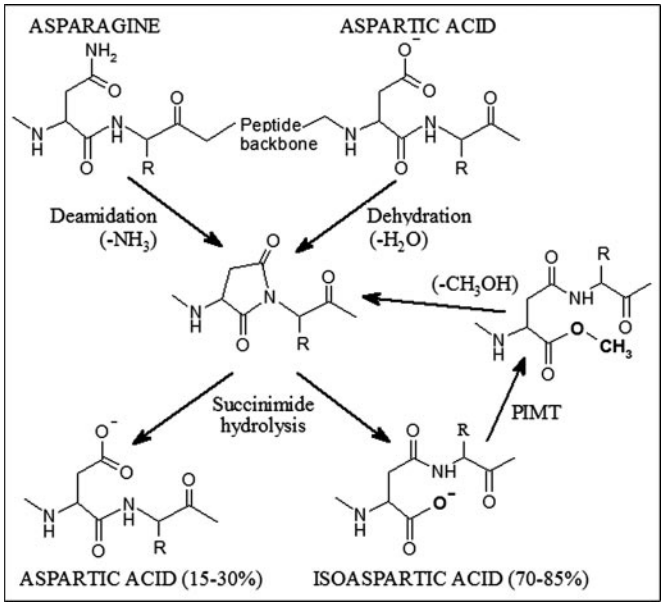

FIGURE 1. **Generation of isoaspartate and PIMT-catalyzed amino acid repair.** Deamidation of an asparagine residue and dehydration of an aspartic acid residue generates a five-membered L-succinimide ring within the peptide chain. Ring opening by hydrolysis produces either an aspartic acid (minor product) or an isoaspartic acid (major product). The carboxyl group of the isoaspartate is methylated by PIMT (indicated in *bold*) utilizing *S*-adenosylmethionine, which is converted to *S*-adenosylhomocysteine in the process. The isoaspartyl methyl ester formed is relatively unstable and is rapidly hydrolyzed, liberating methanol and regenerating the succinimide ring, which can then repeat the cycle. After several rounds of PIMT-catalyzed methylation the majority of isoaspartate can be converted back to aspartate, which can be concomitant with a return of peptide/protein function. Additionally, racemization of the succinimide and its hydrolysis (not shown) produces low levels of D-succinimide, D-isoaspartic acid, and D-aspartate, the latter of which is also a substrate for PIMT.

imide form. Subsequent hydrolysis to aspartate or isoaspartate produces either a repaired or as yet unrepaired peptide linkage, respectively (Fig. 1). Albeit somewhat inefficiently, several rounds of PIMT methylation will reconvert the isoaspartate to aspartate, a process that can be concomitant with restoration of enzymatic function in model proteins and peptides that have been aged *in vitro* or *in vivo* (5–12).

The generation of *Pcmt1*$^{-/-}$ mice has provided an invaluable insight into the physiological consequences of isoaspartate formation. These mice accumulate higher levels of isoaspartate, relative to their wild-type littermates, in all tissues that normally express the enzyme (13–15). *Pcmt1*$^{-/-}$ mice have abnormal neuronal excitability, and most die from an epileptic seizure at less than 2 months of age (13, 14, 16). They experience aberrant mossy fiber-CA3 region synaptic neurotransmission, vacuolar degeneration at the axon hillock of dentate cells, and disorganized microtubules within the dendrites of pyramidal neurons (14, 17). Although smaller on average than their wild-type littermates, the *Pcmt1*$^{-/-}$ mice also have a progressive increase in brain size linked to alterations in the phosphatidylinositol 3-kinase/protein kinase B signaling pathway (14, 16, 18, 19).

To better understand how isoaspartyl residues contribute to these defects, the primary *in vivo* substrates for PIMT must first be determined. Two main approaches have been used to limit isoaspartate repair and allow the substrates to accumulate to a detectable level: inhibition of PIMT (as well as other *S*-adenosylmethionine-dependent methyltransferases) in cultured cells using periodate-oxidized adenosine, and the generation of *Pcmt1*$^{-/-}$ mice. Both techniques produced unrepaired proteins that have been identified by subsequent methylation by exogenous PIMT and radioactive *S*-adenosylmethionine (AdoMet). In this way, histone H2B (20), synapsin 1 (15, 21), tau protein (14), calmodulin (21–22), and tubulin (23–25) have thus far been shown to be physiological PIMT substrates.

Identification of damaged proteins labeled with [^{3}H]AdoMet has been hindered by the instability of the methyl esters and the low levels of methylatable residues even in tissues from *Pcmt1*$^{-/-}$ mice. To minimize these problems, we have used conditions that maintain base-labile methyl esters generated by exogenous PIMT on proteins from *Pcmt1*$^{-/-}$ tissues and employed a rapid and sensitive microchannel plate device to detect methylated proteins resolved by both 1D SDS-PAGE and 2D PAGE. We were able to identify nine new *in vivo* substrates for PIMT from brain tissue: microtubule-associated protein-2, calreticulin, clathrin light chains a and b, ubiquitin carboxyl-terminal hydrolase L1, phosphatidylethanolamine-binding protein, stathmin, β-synuclein, and α-synuclein. The methylation of these proteins suggests a role for PIMT in the maintenance of the neuronal cytoskeleton and regulation of neuronal signaling.

EXPERIMENTAL PROCEDURES

Materials—IPG strips (pH 4–7; 7- and 17-cm lengths) were purchased from Bio-Rad, with all isoelectric focusing performed using a Bio-Rad Protean isoelectric focusing cell. NuPAGE Novex pre-cast gels (4–12% Bis-Tris gels for 1D SDS-PAGE and 4–12% Bis-Tris Zoom gels for 2D PAGE analysis), MES-SDS running buffer, transfer buffer, SeeBlue Plus2 prestained gel standards, and Safe stain were all obtained from Invitrogen. Dithiothreitol (DTT), iodoacetamide, MES, HEPES, wide range molecular weight markers, glycine, glutaraldehyde, and all SDS-PAGE reagents were purchased from Sigma. Isoquant isoaspartate detection kits were purchased from Promega. *S*-Adenosyl-L-[*methyl*-^{3}H]methionine (37 MBq/ml), destreak reagent, and PlusOne silver staining kit were purchased from Amersham Biosciences. Bovine recombinant PIMT provided with the Isoquant kit was used for methylations of homogenates analyzed by 1D and 2D PAGE. This enzyme has a specific activity of ~5000 pmol of methyl groups transferred/min/mg when assayed for trichloroacetic acid-precipitable counts into bovine γ-globulins (Sigma Cohn fraction II) (26), an activity comparable to that produced by recombinant human PIMT (27) when assayed under identical conditions, and similar to that for PIMT purified directly from bovine brain (26).

Mice—Wild-type (*Pcmt1*$^{+/+}$) and PIMT knock-out (KO) mice (*Pcmt1*$^{-/-}$) were generated according to previously detailed procedures and breeding conditions (13, 16). Comparisons in all studies involved either male or female littermates.

Preparation of Brain Extracts—Brains were removed immediately from sacrificed animals and weighed, and crude cytosolic extracts were prepared according to Lowenson *et al.* (28).

Protein concentrations in all extracts were determined using the DC Protein Assay kit (Bio-Rad), with bovine serum albumin as a standard.

Quantitation of Isoaspartate Levels—The levels of isoaspartate in tissue extracts were quantified by a methanol diffusion assay using an Isoquant kit according to the manufacturer's instructions. Briefly, extracts were methylated with recombinant bovine PIMT (Promega, 1.9 μM final concentration) utilizing 20 μM [^{3}H]AdoMet (1 μCi/reaction, 2220 dpm/pmol final specific activity), in a buffer of 100 mM sodium phosphate, pH 6.8, containing 1 mM EGTA, 0.16% Triton X-100, and 0.004% sodium azide (final concentrations) for 30 min at 30 °C. Methylation was terminated, the methyl esters were hydrolyzed by CAPS (pH 10) (with 5% SDS, 2.2% methanol, 0.1% *m*-cresol purple), and the samples retained on ice for 10 min. 50 μl from each of the samples was then spotted onto a sponge inserted into the cap of a scintillation vial. The samples were incubated for 60 min at 40 °C to volatilize [^{3}H]methanol from the labeled proteins into 10 ml of scintillation fluid, which was then counted for radioactivity. Each assay was performed in duplicate from which an average was determined. 50 pmol of isoaspartate-containing delta sleep-inducing peptide provided with the Isoquant kit was similarly methylated to provide a reference level of isoaspartate methylation from which methylation of the cytosolic proteins was quantified.

1D SDS-PAGE Separation of Proteins—Protein extracts were methylated in a final volume of 20 μl in a buffer of 50 mM K-MES, pH 6.2, containing 20 μM [^{3}H]AdoMet (1.5 μCi/reaction, 8250 dpm/pmol final specific activity). Methylation was initiated by the addition of 5 μl of exogenous recombinant bovine PIMT (Promega, 2.4 μM final concentration) and incubated for 30 min at 30 °C. Methylation was terminated by the addition of a quarter of a volume of 5× concentrated reducing solution (10% SDS and 500 mM DTT), and the samples were heated for 10 min at 50 °C. One quarter of a volume of 5× Laemmli sample buffer was added (250 mM Tris/HCl, pH 6.8, 40% (v/v) glycerol, 5% (w/v) SDS, 0.005% (w/v) bromphenol) and proteins (typically 20 μg/gel lane) were resolved on 4–12% Bis-Tris gels for 2 h at 125 V using MES running buffer (pH 7.3) run in an X Cell surelock gel tank (Invitrogen). Proteins were then electroblotted at 80 V for 2 h onto a PVDF membrane (Millipore) using NuPage Transfer buffer (pH 7.2). Membrane-bound protein was stained with Coomassie Blue (Safestain) for 30 min at room temperature and then further fixed by drying overnight. The membranes were destained with 50% methanol (v/v), 10% acetic acid (v/v), and then extensively washed with 20 mM K-MES, pH 6.2. Membrane-bound protein was cross-linked by incubation with 0.5% glutaraldehyde (v/v) in 20 mM K-MES pH 6.2 overnight. Membranes were again washed with 20 mM K-MES, pH 6.2, and then residual unreacted glutaraldehyde blocked by incubation with 0.2 M glycine in 20 mM K-MES pH 6.2 for 4 h at room temperature. Blots were finally washed as before and left to dry before application of ^{14}C markers onto the positions of the molecular weight standards. Blots were applied to a Microchannel Plate device and autoradiographed for 7 or 24 h (refer to Fig. 3) to visualize radioactive targets (29).

Equivalent gels to those described above were stained with either colloidal Coomassie Brilliant Blue (Invitrogen) overnight or with silver (Amersham Biosciences PlusOne kit) according to the manufacturer's instructions to provide comparisons of protein expression in the *Pcmt1*$^{+/+}$ and *Pcmt1*$^{-/-}$ tissues. Stained gels were either photographed using a Fuji digital camera or scanned using an Agfa Duoscan T1200 flatbead scanner. Radiolabeling and 1D SDS-PAGE were performed on five different pairs of littermates for brain tissue, and three different pairs of littermates for all other tissues.

2D PAGE Separation of Proteins—Methylation was performed similarly to that for 1D SDS-PAGE (but scaled up to 600 μg/analysis), terminated by the addition of 700 μl of protein precipitation solution (acetone:diethyl ether (2:1 (v/v)), and samples were placed on ice. Precipitated proteins were collected by centrifugation at 5000 rpm for 3 min. The precipitate was washed three times with ether:industrial methylated spirit: water (10:7:2, v/v) and air-dried, and then proteins were dissolved in a rehydration buffer (9.8 M urea, 2% (w/v) CHAPS, 0.5% IPG buffer) containing 12 μl/ml of the anti-oxidant destreak reagent, at room temperature for 1 h. The solubilized protein was actively rehydrated into either 7- or 17-cm, pH 4–7 IPG isoelectric focusing strips for 16 h at 50 V, and then focused for 16 h according to the manufacturer's guidelines for each strip. Focused strips were washed in an equilibration buffer of 0.375 M Tris/HCl, pH 6.8, 6 M urea, 2% SDS, 20% glycerol, containing 2% (w/v) DTT for 10 min, and then similarly washed with the same buffer except 2.5% (w/v) iodoacetamide replaced DTT. After this reduction and alkylation, strips were equilibrated in MES running buffer before protein separation by SDS-PAGE. Strips of 7-cm length were resolved in the second dimension using Zoom gels. Strips of 17 cm were layered onto freshly prepared 5–20% (w/v) acrylamide gradient gels, and proteins were resolved at a constant current of 22 mA for 20 h within a Protean II xi 2D cell (Bio-Rad). Proteins were then transferred to a PVDF membrane and autoradiographed for 16–24 h under conditions described for 1D SDS-PAGE. Equivalent 2D PAGE gels were stained with either colloidal Coomassie or silver, and an autoradiographic template was used to locate spots of interest for mass spectrometry. Brain tissue 2D maps were typically generated two or three times from each of five different pairs of littermates.

MALDI-TOF Mass Spectrometry—Stained protein spots were excised and transferred into a 96-well plate using an automated MassPrep robotic system (ProteomeWorks-Bio-Rad). Gel pieces were destained, and then reduced and alkylated with DTT and iodoacetamide before tryptic digestion *in situ*. Tryptic peptides were desalted by binding and then elution from a C18 Zip-tip (Millipore), and then they were mixed with α-cyano-4-hydroxycinnamic acid (Sigma C-2020) matrix and analyzed by MALDI-TOF mass spectrometry (Micromass MALDI, Waters, UK). A number of intact singularly charged peptides were identified, and the masses were used in a search algorithm (MASCOT peptide mass fingerprint) to screen several protein databases, including SwissProt for peptide mass matches to enable protein identification.

LC MS/MS—Stained protein spots were excised, reduced, and alkylated, and tryptic peptides were produced according to the MALDI method. Extracted tryptic peptides were then run on a Waters QTOF2 hybrid quadrupole mass spectrometer

incorporating an integrated capillary LC system. Tryptic digestion products were initially loaded onto a C18 pre-column for desalting and then eluted onto an analytical capillary C18 column (100-mm × 0.75-mm internal diameter). The LC system incorporated a flow splitting device to give a final flow through the column of 200 nl/min. Typically, a solvent gradient was run over a total of 1 h to elute peptides from the capillary column and re-equilibrate prior to loading the next sample.

Eluted peptides from the analytical column were directly submitted into the mass spectrometer via a nanosprayer device attached to the outflow from the LC system and operating at 3 kV. In addition, a reference solution containing a peptide of known mass was sprayed into the mass spectrometer from a separate sprayer. This ion source was sampled at regular intervals throughout the run to assist in maintaining accurate mass measurements of the ionized peptides from the analyte spray. Data-dependent switching was incorporated so that whenever a peptide with an associated charge of 2+ or 3+ was detected above a preset threshold signal, the mass spectrometer would automatically switch to MS/MS mode to generate fragmentation data from the detected peptide.

Software was enabled to scan over multiple channels to simultaneously fragment up to three co-eluting peptides and collect the fragmentation data from each one individually. A preset range of collision voltages was set up in the method to fragment each peptide as efficiently as possible. Raw data files were analyzed using MassLynx 4.0 (incorporating BioLynx) and ProteinLynx Globalserver 2 (Waters) to assess the identities of proteins present in the digest. The peak list file generated from ProteinLynx Globalserver 2 analysis was also used in alternative search engines accepting this format of data file, including MASCOT. In addition, some of the fragmentation data were analyzed manually, and *de novo* sequencing was carried out on selected peptides.

Immunoprecipitation of MAP-2—Methylation of protein extracts were performed similarly to that for 1D SDS-PAGE but with 160 μg of protein used from each genotype. After methylation, samples were placed on ice, and then precleared by rotation with normal rabbit IgG-agarose conjugate (sc-2345, Santa Cruz Biotechnology, Santa Cruz, CA) for 1 h at 4 °C. MAP-2 polyclonal antibody was then added (0.6 μg of sc-20172, Santa Cruz Biotechnology) for 1 h at 4 °C. Protein A-agarose (sc-2001, Santa Cruz Biotechnology) was added for 45 min at 4 °C to capture immune complexes. The agarose beads were then pelleted by centrifugation and washed five times with an immunoprecipitation (IP) wash buffer of 20 mM K-MES, pH 6.2, containing 150 mM NaCl and 0.05% Tween 20. Washed beads were rehydrated in 20 μl of 20 mM K-MES, pH 6.2, and 5× concentrated reducing solution (10% SDS and 500 mM DTT) added, and the samples were heated for 10 min at 50 °C. One-quarter of a volume of 5× Laemmli sample buffer was added, and proteins which were liberated from the antibody separated by 1D SDS-PAGE as described previously. Proteins were then transferred to a PVDF membrane and autoradiographed for 24 h.

Western Blotting—Blots prepared from the MAP-2 immunoprecipitation were washed with IP wash buffer and then incubated in a blocking buffer (IP wash buffer containing 5% (w/v) milk fat) for 1 h at room temperature. Blots were incubated with MAP-2 antibody (sc-20172), at a 1:2000 dilution in blocking buffer for 2 h at room temperature, washed with IP wash buffer, and then incubated with secondary antibody (polyclonal goat anti-rabbit immunoglobulins-horseradish peroxide-conjugated, Dako, P0448) for 1 h at room temperature. Blots were further washed with IP wash buffer, then MAP-2 immunolocalization visualized using ECL (Pierce), and captured on CL-Xposure x-ray film (Pierce). Films were scanned on an Agfa Duoscan T1200 flatbead scanner.

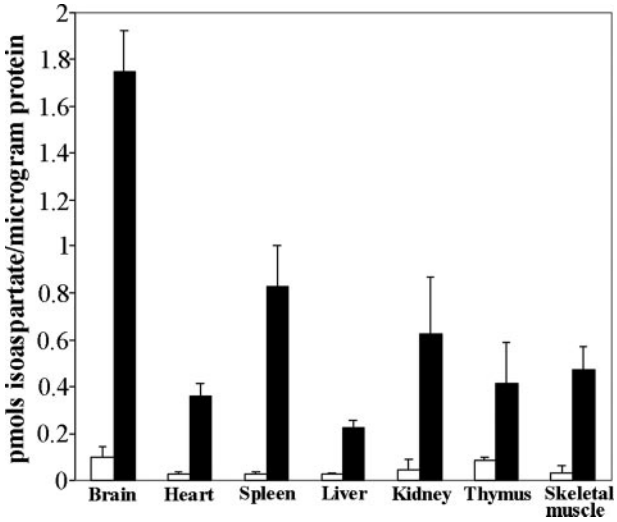

FIGURE 2. **Quantitation of tissue isoaspartate levels in *Pcmt1*$^{+/+}$ and *Pcmt1*$^{-/-}$ mice using a methanol diffusion assay.** The isoaspartate content of tissue homogenates from *Pcmt1*$^{+/+}$ (*open columns*) and *Pcmt1*$^{-/-}$ (*shaded columns*) mice was quantified using an Isoquant kit. Three pairs of littermates were used for all tissues except brain, for which five pairs of littermates were analyzed. Standard deviation *error bars* are included for each analysis.

RESULTS

PIMT Knock-out Mice Accumulate Higher Levels of Isoaspartate Than Wild-type Littermates—We determined the isoaspartate content of protein in seven tissues from both wild-type and PIMT KO mice using an Isoquant kit. In the absence of PIMT activity, all tissues examined, including brain, heart, spleen, liver, kidney, thymus, and skeletal muscle, accumulated higher levels of isoaspartyl residues than those of their wild-type littermates (Fig. 2). Brain homogenate from PIMT KO mice exhibited the highest levels of isoaspartate, having close to 2 pmol of isoaspartate/μg of protein, an ~18-fold increase over wild type. By comparison, homogenates of the other assayed KO tissues ranged from 0.2 pmol of isoaspartate/μg of protein in liver to 0.8 pmol of isoaspartate/μg of protein in spleen.

1D SDS-PAGE Shows a Variety of Different PIMT Substrates in Pcmt1$^{-/-}$ *Tissues*—Tissue homogenates from wild-type and KO mice were methylated with [^{3}H]AdoMet and exogenous PIMT, and the proteins were separated by 1D SDS-PAGE using separation conditions designed to minimize the loss of base-labile methyl esters. Proteins were electroblotted onto a PVDF membrane and then exposed to a Microchannel Plate autoradiographic detector. The solutions described under "Experimental Procedures" restricted the proteins to conditions of no higher than pH 7.3.

An autoradiographic exposure for 7 h (Fig. 3*A*) showed that, in agreement with the isoaspartate quantitation described

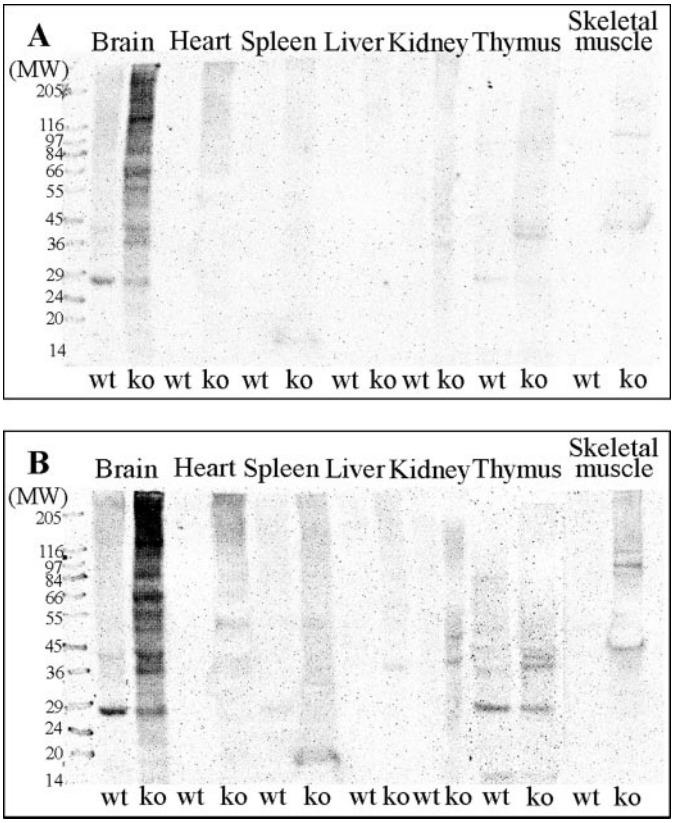

FIGURE 3. **Mouse tissue PIMT protein substrate resolution by 1D SDS-PAGE.** *A*, 20 μg of protein from tissue homogenates of *Pcmt1*$^{+/+}$ (wild-type (*wt*)) and *Pcmt1*$^{-/-}$ (knock-out (*ko*)) mice littermates were methylated with [^{3}H]AdoMet using exogenous PIMT, and proteins were resolved by 1D SDS-PAGE. Proteins were transferred to a PVDF membrane, and PIMT substrates were visualized by autoradiography for either 7 h (*A*) or 24 h (*B*).

above, *Pcmt1*$^{-/-}$ brain tissue accumulates higher levels of isoaspartate-containing proteins than do the other tissues. This autoradiograph also demonstrated that *Pcmt1*$^{-/-}$ brain tissue accumulates isoaspartate into numerous protein bands, present across a broad range of molecular weights.

Specific PIMT substrates were distinguished by an increase in their *in vitro* radiolabeling when extracts were prepared from KO relative to wild-type tissues. Fig. 3*A* shows that relatively few proteins (*e.g.* the 27-kDa species) in wild-type tissues arise from the activity of an endogenous methyltransferase that also utilizes AdoMet as a methyl donor, or are labeled by exogenous PIMT at isoaspartyl residues that are not accessible to endogenous PIMT *in vivo*, and thus the labeling of these bands do not increase in KO tissue.

Although PIMT targets were abundant enough in *Pcmt1*$^{-/-}$ brain extracts to be observed after only 7 h of autoradiography, this was not a long enough exposure to detect many of the PIMT substrates in the other tissues. Increasing the autoradiographic exposure to 24 h (Fig. 3*B*), however, made these PIMT targets more distinct allowing their characterization by denatured molecular weight (supplemental Table S1). As in brain, these targets are present across a wide range of molecular weights, but the combination of major substrate proteins in each tissue appears to be quite distinct, and thus may primarily be proteins that are unique to each tissue. The most noteworthy exception to this is the presence of a PIMT protein target(s) of molecular masses 36–39 kDa resident within all tissues examined.

Two-dimensional PAGE Resolved Numerous Brain PIMT Substrate Proteins—The relative abundance of PIMT substrate proteins favored brain tissue for further substrate characterization and identification. 2D PAGE is a useful method for isolating many proteins at once, but at a pH above 8 rapid hydrolysis of methyl esters occurs, and hence no major recovery of radiolabeled PIMT substrates can be achieved. We therefore limited our analyses to proteins with pI values between 4 and 7, which could survive isoelectric focusing within immobilized gradients of pH 4 to 7 with their methyl esters intact. Following subsequent 1D SDS-PAGE separation, equivalent gels were stained with colloidal Coomassie Blue (Fig. 4*A*, *upper panels*) or electroblotted and autoradiographed (Fig. 4*A*, *lower panels*).

The composition of the cytosolic protein recovered from brain tissues, as judged by Coomassie staining of the 2D PAGE gels, was similar for the two genotypes. The most prominent radiolabeling in the wild-type extract was in the area at a pI of 4.3–4.5, ranging from ~70 kDa to above the 188-kDa protein marker. A corresponding region in the KO autoradiographs was even more heavily labeled, but many other proteins from the KO tissue were also labeled (Fig. 4*B*).

Two-dimensional analysis of radiolabeled proteins from five pairs of littermates was undertaken. The major PIMT-radiolabeled protein spots/regions were consistent in all *Pcmt1*$^{-/-}$ mice examined, and we have presented representative autoradiographs from three different *Pcmt1*$^{-/-}$ mouse brain extracts in Fig. 4*B*.

Twenty-seven spots/radiolabeled regions were observed in the ^{3}H-methylated PIMT KO tissues. These have been characterized according to their molecular weight and pI and have been numbered sequentially in order of descending molecular weight (Fig. 4*C* and supplemental Table S2).

It is apparent that the migration of some of the Coomassie-stained protein spots correlate perfectly with a radioactive counterpart; several of these have been marked with *arrows* in Fig. 4*A*. These protein spots were excised and analyzed by mass spectrometry peptide fingerprinting, and the results are summarized in Table 1.

Additionally, we improved the resolution of the relatively low molecular mass protein spots (below the 28-kDa protein marker) using immobilized pH gradient strips of increased length (17-cm strips rather than 7 cm, again with a pH gradient of between 4 and 7). These isoelectric focused proteins were then separated in the second dimension using 5–20% acrylamide gradient gels. The proteins were then visualized with more sensitive silver staining, and PIMT substrate proteins (identified from a radiolabeling template) were eluted for mass spectrometry identification. Fig. 5 shows a typical silver-stained gel of these well resolved low molecular weight proteins from which the PIMT substrate proteins (numbered according to Fig. 4*C*) were excised and mass was analyzed. Protein *spot 17a* was visible by silver staining but was at a level too low for mass identification. It is assumed to be a further post-translationally modified form of *spots 17b–d*. The proteins identified as a result of these larger IPG strips are included in Table 1.

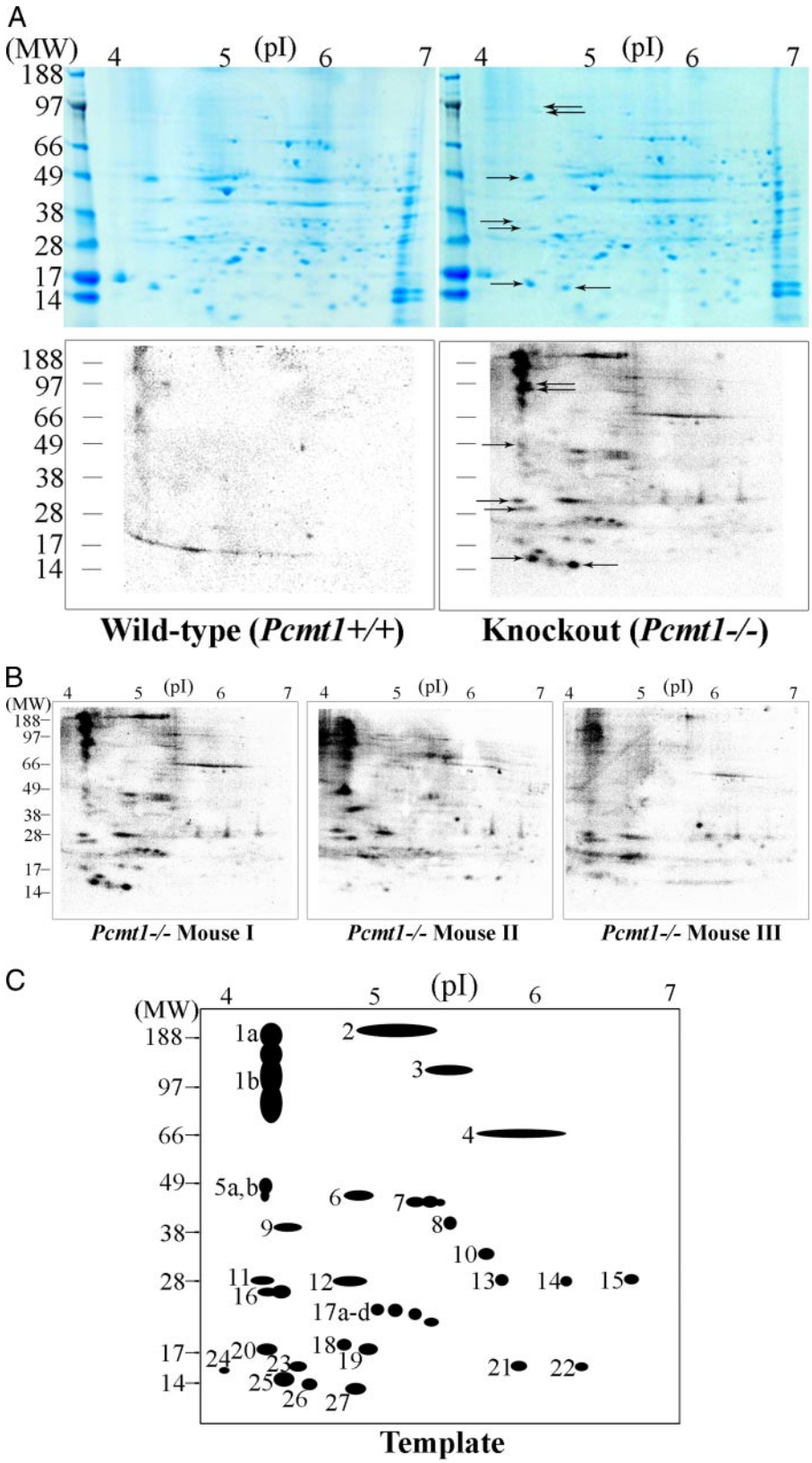

FIGURE 4. **Separation of brain PIMT substrates by 2D PAGE using 7-cm IPG strips.** *A*, 600 μg of protein from brain homogenates of *Pcmt1*$^{+/+}$ and *Pcmt1*$^{-/-}$ mouse littermates was separated by 2D PAGE using 7-cm pH 4–7 IPG strips, and proteins were stained with colloidal Coomassie (*upper panels*), or radiolabeled with [^{3}H]AdoMet using exogenous PIMT, transferred to PVDF membranes, and exposed for 16 h of autoradiography (*lower panels*). Some of the Coomassie-stained proteins had a clear corresponding radiolabeled counterpart (marked with *arrows*). *B*, 600 μg of protein from brain homogenates from two additional *Pcmt1*$^{-/-}$ mice was radiolabeled with exogenous PIMT, separated by 2D PAGE using 7-cm IPG strips, and autoradiographed, and they are shown with the KO mouse from *panel A*. *C*, *Pcmt1*$^{-/-}$-radiolabeled protein spot migrations provided a means to produce a template for calculations of approximate denatured molecular weight and estimated pI for the major recurring PIMT substrates.

TABLE 1

Identification of major mouse brain PIMT substrates

Mouse brain PIMT substrate proteins characterized by 2D PAGE were identified by mass spectrometric analysis of tryptic fragments from gel spots. Tryptic fragment coverage from MALDI MS of the identified proteins are shown, from which a MASCOT probability score was generated. A probability score of above 65 for MALDI analysis was a significant match ($p < 0.05$) of tryptic peptides to those within protein databases such as Swiss-Prot. In addition, or alternatively, LC MS/MS was performed where indicated, and an example of the one or more sequenced peptides that confirmed protein identification was detailed. Predicted molecular masses (in kDa) and theoretical isoelectric point (pI) values are also included.

Spot no.	Protein identification	Tryptic fragment coverage	MASCOT probability score	Peptide(s) verified by LC MS/MS	UniProtKB/Swiss-Prot entry	Protein mass	pI
		%				*kDa*	
1a	MAP-2	10	192	ND[a]	P20357	199	4.80
1b, 5a	β-Tubulin(s)	46	ND	Ala^{63}–Lys^{103} Leu^{217}–Arg^{251}	P68372	50	4.79
	α-Tubulin	23	ND	Leu^{230}–Arg^{243}	P68369	50	4.94
5b	Calreticulin	38	166	ND	P14211	48	4.33
11, 16	Clathrin light a	16	118	Leu^{102}–Arg^{110}	O08585	26	4.45
	Clathrin light b	25	111	Leu^{114}–Lys^{122} Glu^{182}–Lys^{204}	Q61RU5	25	4.56
17b–d	UCHL1	48	138	Asn^{136}–Arg^{153}	Q9R0P9	25	5.14
18, 19	PEBP	45	106	ND	P70296	21	5.19
21, 22	Stathmin	35	77	Ala^{14}–Arg^{26} Asp^{43}–Arg^{59} Ala^{85}–Lys^{94}	P54227	17	5.95
24	Calmodulin	35	ND	Glu^{14}–Arg^{37} Met^{76}–Arg^{86} Val^{91}–Arg^{106}	P62204	17	4.09
25	β-Synuclein	38	87	Glu^{13}–Lys^{21} Gln^{24}–Lys^{57} Glu^{60}–Lys^{84}	Q91ZZ3	14	4.38
27	α-Synuclein	44	125	Glu^{46}–Lys^{58} Glu^{61}–Lys^{80} Thr^{81}–Lys^{96}	O55042	14	4.74

[a] ND, not determined.

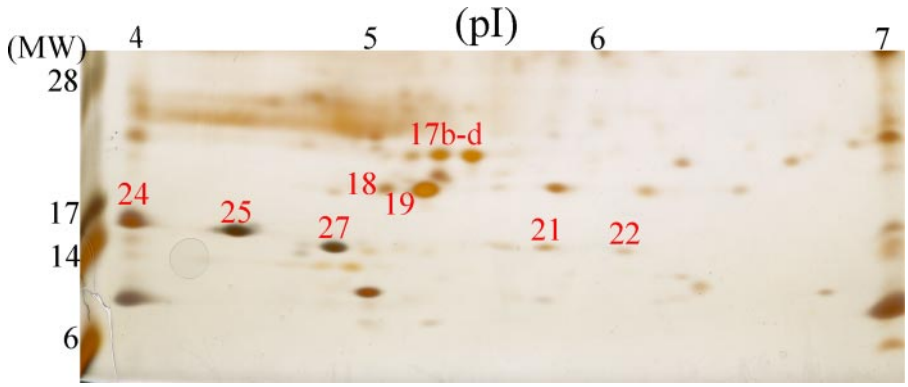

FIGURE 5. **Separation of brain PIMT substrates by 2D PAGE using 17-cm IPG strips.** 600 μg of brain homogenate protein from a *Pcmt1*$^{-/-}$ mouse was separated by 2D PAGE using a 17-cm pH 4–7 IPG strip, and proteins were stained with silver. The gel region comprising the relatively low molecular mass brain proteins (below the 28-kDa protein marker) is shown from which PIMT substrate proteins (labeled according to Fig. 4*C*) were excised for mass analysis.

Silver-stained gels were also generated from brain homogenates from *Pcmt1*$^{+/+}$ mice to provide a direct comparison of protein staining levels with brain homogenates from *Pcmt1*$^{-/-}$ littermates. There were no significant changes to the levels of staining of the proteins identified to be PIMT targets evident between the genotypes, suggesting these proteins were not up- or down-regulated in their production in the KO mice brains (results not included). Additionally, mass spectrometry analysis was also performed on these *Pcmt1*$^{+/+}$ mice, and protein identifications were found to be identical to their *Pcmt1*$^{-/-}$ counterparts, indicative of a single protein present that was not being masked by a co-migratory protein elevated in expression in the KO mice (results not shown).

Immunoprecipitation of MAP-2—Our methodology for 2D PAGE separation of brain extracts has enabled us to identify novel substrates for PIMT based upon the co-localization of methylated and non-methylated counterparts. As a supplemental validation of this technique, we radiolabeled brain extract from both wild-type and PIMT KO mice using [^{3}H]AdoMet and exogenous PIMT, and immunoprecipitated one of our proposed PIMT protein targets, MAP-2, using specific MAP-2 antibodies.

MAP-2 expression levels were similar in each genotype by Western blot analysis, the antibody recognizing several of what are presumed post-translationally modified forms of MAP-2. Recovery of MAP-2 by immunoprecipitation was also similar in either case (Fig. 6, *left panel*). However, after autoradiography, only from the KO mice was significant radioactivity (isoaspartate labeling) recovered, which co-distributed with immunoprecipitated MAP-2 protein (Fig. 6, *right panel*), thereby confirming that this protein accumulated isoaspartate as a result of *Pcmt1* gene knock-out.

DISCUSSION

To gain insight into the physiological role of the protein repair enzyme PIMT, we used a proteomic strategy to identify the primary substrates for this methyltransferase in mice. First, however, we characterized tissues richest in isoaspartate using the Isoquant assay. Examination of seven tissues from PIMT KO and wild-type mice showed that *Pcmt1*$^{-/-}$ brain had more than twice the isoaspartyl residues per unit protein found in

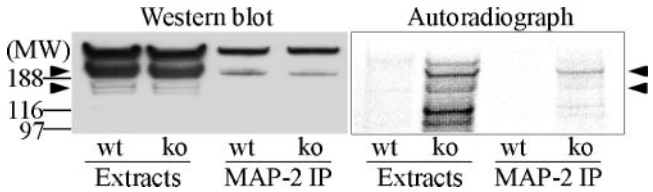

FIGURE 6. **MAP-2 Western blot and immunoprecipitation.** 160 μg of protein from tissue homogenates of *Pcmt1*$^{+/+}$ (wild-type (*wt*)) and *Pcmt1*$^{-/-}$ (knock-out (*ko*)) mice littermates were methylated with [^{3}H]AdoMet using exogenous PIMT. 20 μg of these radiolabeled extracts was resolved by 1D SDS-PAGE. MAP-2 was immunoprecipitated from the remaining 140 μg, and MAP-2 immune complexes were also resolved by 1D SDS-PAGE. Protein was transferred to a PVDF membrane, and extracts and the immune complexes were Western blotted for MAP-2 protein (*left panel*), and autoradiographed for 24 h (*right panel*). Co-localization of MAP-2 protein in extracts and immunoprecipitates with radiolabeled counterparts are marked with *arrowheads*.

other tissues, and more than 15-times the damaged residues in tissues from wild-type littermates, as has been observed previously (13–15).

Identification by mass spectrometry of proteins separated by 2D electrophoresis has recently become a widespread method of proteomic analysis. It has not been used for the analysis of PIMT-methylated proteins, however, because isoaspartyl methyl esters undergo rapid spontaneous hydrolysis at basic pH, a property exploited by the isoaspartate quantitation assay described above (Fig. 2). Because the standard SDS-PAGE developed by Laemmli (30) involves casting and running the gel at a pH above eight, isoaspartyl methyl esters can be lost during this procedure.

To avoid base-driven methyl-ester loss, an alternative acidic (pH 2.4) SDS-PAGE separation system has been used to detect PIMT substrates (20, 31), but these acidic conditions result in relatively poor protein resolution. Recently, Aswad and colleagues have improved the resolution of PIMT substrates (20, 21) using Novex NuPage gels, which are cast at pH 6.4 and run with a pH 7.3 buffer. We have now further enhanced this procedure first by coupling isoelectric focusing between pH 4 and 7 to this near neutral pH molecular weight separation, and then by analyzing the radiolabeled methylated proteins transferred to a PVDF membrane using a Microchannel Plate autoradiographic imager (29, 32). The sensitivity of this Microchannel Plate device is superior to conventional film autoradiography; it can image, in real-time, as little as 0.1 Bq/mm^2, and has a broad linear dynamic measurement range (greater than six orders of magnitude), traits well suited to detection of low level radiolabeling even after relatively short autoradiographic exposure times (32, 33).

Having developed this methodology for maintaining methyl esters during protein separation, we were able to track PIMT target proteins by their increased *in vitro* methylation when isolated from PIMT KO mice compared with wild-type littermates. The PIMT substrates were initially characterized by 1D SDS-PAGE, and we found that these proteins were present across a broad range of molecular weights. It is noteworthy that the primary substrates for PIMT are mostly different in each tissue, presumably reflecting tissue-specific protein expression and function. The future identification of the major PIMT substrates in these mouse tissues will certainly be of interest.

It is also striking how prominent the damaged proteins are in *Pcmt1*$^{-/-}$ brains compared with other tissues. The fact that *Pcmt1* message expression (34) and enzyme activity (13) are both particularly high in mouse brain suggests that either the presence of elevated repair activity has allowed for the evolution of proteins that are particularly susceptible to isoaspartate formation or that PIMT levels are responsive to the levels of damaged proteins.

Separation of *in vitro* ^{3}H-methylated proteins from *Pcmt1*$^{-/-}$ mouse brains using pH 4–7 2D PAGE and analysis of the radiolabeled spots by mass spectrometry have enabled us to identify nine new brain substrates for PIMT: microtubule-associated protein-2, calreticulin, clathrin light chains a and b, ubiquitin carboxyl-terminal hydrolase L1, phosphatidylethanolamine-binding protein, stathmin, β-synuclein, and α-synuclein.

Although carboxyl methylation can change the mass and pI of a protein, the proteins identified here are presumably those in which this labeling does not significantly alter the pI of the protein from its isoaspartate-containing counterpart. Further, it is possible that a minor protein that is an excellent PIMT substrate may co-resolve with an abundant protein that is itself not methylated. Additionally, there may be some proteins up-regulated in *Pcmt1*$^{-/-}$ mice relative to their wild-type littermates which could also overlay true PIMT targets by protein co-migration, or reflect increased production of proteins that contain isoaspartate but are normally inaccessible to PIMT. However, by restricting the majority of our mass spectrometry analyses to single silver-stained proteins, which were present to similar levels in both wild-type and KO mice, we would expect to have avoided many co-migratory proteins, because, if they are present, they would probably enhance silver staining and contribute to peptide masses identified by MALDI, or peptide sequences resolved by LC MS/MS, and thereby provide alternative protein assignments.

A MASCOT probability score was generated from the MALDI MS tryptic fragment data for each proposed PIMT target. MASCOT provides a probability-based scoring system that assesses the significance of matches between peptides of an experimental sample and those from a protein data base. Using our peptide mass parameters, a MASCOT probability score of >65 is considered significant (a matching event, which would occur at random with a frequency of $<5\%$ ($p < 0.05$)); hence all of our proposed PIMT targets had a relatively high confidence in their protein assignments. However, because our MALDI mass analysis is conducted within the mass range of 800–3000 Da, proteins that do not liberate many peptides within this screening mass range can be under-represented; hence the lower (but still significant) MASCOT scores for stathmin and β-synuclein. To further validate these two PIMT targets, and to provide additional support for the identification of some of the other proposed PIMT targets, we have performed LC MS/MS analyses (Table 1). LC MS/MS sequenced additional tryptic fragments outside of the MALDI mass screening range and, thereby, enabled us to substantiate our MALDI MS findings and identify the other PIMT targets, calmodulin and tubulin.

Our proteomic results were further validated by an independent methodology, that of specific immunoprecipitation of one of our proposed PIMT targets, MAP-2. After radiolabeling brain extracts from both wild-type and PIMT KO mice, immunopre-

cipitation of MAP-2 resulted in significant recovery of co-localized radioactivity with MAP-2 protein only from the KO extracts, indicative of isoaspartate accumulation within this protein as a result of *Pcmt1* gene removal. Further definitive analysis will also be required for the other PIMT substrate proteins identified, and their site(s) of methylation identified.

In vitro and *in vivo* experiments have demonstrated that aberrant isoaspartate formation can be concomitant with loss of protein function, and the isoaspartate increase in mice caused by PIMT gene deletion leads to stresses that culminate with a terminal epileptic seizure (5–15, 35). We therefore propose that the isoaspartyl residues that arise in the PIMT targets we have listed above will probably hinder their normal function, and some of these damaged proteins will contribute to the seizure phenotype and histopathological abnormalities of the PIMT KO mice.

α-Synuclein (*spot 27*), a neuronal protein found within presynaptic terminals, is widely distributed throughout the brain but is particularly abundant in the CA3 region of the hippocampus and the mossy fiber terminals of the dentate gyrus (36, 37). Although precise functions of α-synuclein have not been clearly defined, it is thought to have a major role in synaptic vesicle mobilization and neurotransmitter release (36, 38, 39) and an involvement in synaptic plasticity (39, 40). An isoaspartate-rich and therefore presumably less functional α-synuclein is consistent with the phenotypical/histopathological changes associated with the PIMT KO mice, in which the mossy fiber-CA3 neurons have aberrant synaptic transmission and irregular synaptic vesicle distribution and fail to show long term potentiation, actions suggested to be presynaptic in their origin (17, 38).

β-Synuclein (*spot 25*) is a highly homologous member of this synuclein protein family. Like α-synuclein, β-synuclein is concentrated in presynaptic nerve terminals, and is regulated by phosphorylation. The high degree of protein homology and co-localization of α- and β-synucleins suggests their functional redundancy (41, 42). Thus, the increased isoaspartate that arises within β-synuclein in PIMT KO mice may also contribute to irregular synaptic organization and synaptic transmission.

Ubiquitin carboxyl-terminal hydrolase L1 (UCHL1, *spots 17b–d*) is a ubiquitin thiolesterase that is involved in the processing of ubiquitin precursors and the de-ubiquitination of ubiquitinated proteins, including synucleins. As a component of the proteasome system that targets proteins for degradation, alterations in UCHL1 activity within PIMT KO mice could influence numerous neuronal protein turnover and signaling events (43).

Phosphatidylethanolamine-binding protein (PEBP, *spots 18* and *19*, also known as Raf kinase inhibitory protein) is an inhibitor of the Raf/MAPK signaling cascade that drives cellular processes, including growth and differentiation (44, 45). It therefore follows that isoaspartate-rich PEBP may lose some of its ability to inhibit this MAPK pathway, which would result in increased mitotic cell division in some brain regions. Consistent with this proposal, the dentate gyrus, a region of relatively high PEBP expression (46), has been found to have an increased cell number in *Pcmt1*$^{-/-}$ mice compared with wild-type littermates (19). Likewise, a reduction in the inhibitory power of PEBP due to isoaspartyl accumulation might also explain the increased MAPK phosphorylation/signaling reported for PIMT KO lymph nodes (47).

Additionally, the first eleven amino acids of PEBP encompass a bioactive peptide termed hippocampal cholinergic stimulating peptide, which is enzymatically liberated from PEBP in a number of cell types, including hippocampal neurons. This peptide has been suggested to possess a number of regulatory functions, which include influencing acetylcholine synthesis and presumably subsequent neurotransmitter release (48). Thus, the effect of isoaspartyl accumulation on the activity of the peptide must also be investigated.

MAP-2 was found within the area denoted *spot 1a* in Fig. 4. This region is the most intensely methylated in both wild-type and KO 2D PAGE autoradiographs, indicative of a major substrate for PIMT. The finding that MAP-2 accumulates isoaspartyl residues is in agreement with a previous report that a high molecular weight component of microtubules (as well as tubulin itself, *spots 1b* and *5a*) is a substrate for PIMT (23). MAP-2, in concert with other microtubule-binding proteins (including stathmin, see below), influences the dynamics of microtubule polymerization and depolymerization and, thus, neuronal shape, polarity, mobility, and plasticity (49, 50). MAP-2 has been detected mainly in neuronal dendrites (51). Hence, the potential dysregulation of its action due to isoaspartate accumulation might contribute to the disorganized microtubules observed within the dendrites of pyramidal neurons in the PIMT KO mice (14, 17).

Stathmin (*spots 21* and *22*) binds to two α/β tubulin heterodimers, and this binding (and microtubule polymerization inhibition activity) can be regulated by phosphorylation through a number of signaling pathways, including that of nerve growth factor, which stimulates stathmin phosphorylation by a MAPK signaling cascade (52–54). Hence, alteration (due to isoaspartyl residues) in the ability of PEBP to inhibit the MAPK signaling pathway may also impinge upon MAPK downstream signaling targets such as stathmin and MAP-2.

It has been shown that the increase in brain size of PIMT KO mice may result at least in part from alterations in activity of the phosphatidylinositol 3-kinase protein kinase B signaling pathway (18, 19). Protein kinase B influences the activity of p27^{kip1}, which interacts with stathmin to regulate cell cycle progression (55). Thus, stathmin dysregulation also may directly (or indirectly, from alteration of one of its regulatory interacting proteins or signaling cascades) contribute to the altered cellular size and cell division observed within the brains of PIMT KO mice.

Clathrin light chains a and b (*spots 11* and *16*) are major protein components of the endocytotic pits that interact with the microtubular network to ferry and internalize proteins from, and adjacent to, the plasma membrane (56). Clathrin is also present within other endosomal compartments as well as having a cytoplasmic reservoir (57). Nerve terminal synaptic vesicles are recycled by both clathrin-dependent and clathrin-independent mechanisms (58). The accumulation of isoaspartate within clathrin from PIMT KO mice may reduce the efficiency of clathrin-dependent synaptic vesicle recycling and, thereby, subsequent synaptic signaling.

Additionally, the hippocampal mossy fiber-CA3 synapse hyperexcitation reported for the *Pcmt1*$^{-/-}$ mice can be repressed by a γ-aminobutyric acid $(GABA)_A$ receptor agonist, suggesting this synaptic defect arises from reduced activity of GABAergic neurons (17). Further, challenging *Pcmt1*$^{-/-}$ mice with a $GABA_A$ receptor antagonist exasperated the phenotype triggering a major motor seizure (13). $GABA_A$ receptors undergo constitutive clathrin-coated pit endocytosis, which can regulate synaptic inhibition (59). Therefore a disruption of clathrin-coated pit activity due to isoaspartate residues within clathrin light chains a and b may also limit $GABA_A$ receptor recycling and, thereby, contribute to this mossy fiber-CA3 synapse hyperexcitability.

Calreticulin (*spot 5b*) was originally considered to be solely an endoplasmic reticulum (ER) resident protein, where it participates in calcium homeostasis, and has a role as a protein chaperone (60). Recently, a broader cellular distribution for calreticulin has been reported, including cytosolic residency and additional protein functions such as acting as a co-receptor for C1q and as a recognition ligand on apoptotic cells (61). Further study will be warranted to determine the effect of increased isoaspartate on the functions of this protein, but because calcium mobilization can contribute to neurotransmission-signaling events, a defect in calcium homeostasis due to isoaspartate within calreticulin and the calcium-binding protein calmodulin (*spot 24*) could also influence synaptic signaling.

It is noteworthy that two major isoforms of PIMT have been identified as products of alternative splicing: the well characterized PIMT I isoform and PIMT II, which differs from the former isoform in that it possesses an ER retention signal. It has been proposed that this PIMT isoform may therefore specifically function to regulate protein isoaspartate within ER or within another specialized cellular compartment (62), although we have as yet found no evidence that PIMT II possesses a targeting domain for these compartments.[3] Further experiments will be required to specifically evaluate protein targets within the ER, but there remains the possibility that calreticulin within the ER could represent the first PIMT II-specific substrate.

In summary, either individually or, more likely, collectively, the accumulation of isoaspartyl residues in MAP-2, PEBP, UCHL1, stathmin, tubulin, and the microtubule-associated protein tau, would be expected to promote the disorganized cytoskeletal assembly that has been observed in PIMT KO mouse brains (14, 17). Likewise, isoaspartate-rich and potentially dysfunctional α-synuclein, β-synuclein, UCHL1, PEBP, clathrin light chains a and b, calreticulin, calmodulin, and synapsin 1 (a protein whose functions include tethering synaptic vesicles to the cytoskeleton (15, 21, 63)), could drive the aberrant synaptic transmission recorded in these mice (13, 14, 16, 17).

Proteins are generally less soluble at or near their pI, hence the majority of eukaryotic cytosolic proteins have been predicted to possess a pI below neutral, *i.e.* lower than that for the pH of cytosol (64). Our protein coverage between IPG strips of pH 4–7 was therefore likely to be relatively high. However, for the PIMT substrates: synapsin 1 (molecular mass, 74 kDa; theoretical pI, 9.81), and histone H2B (molecular mass, 14 kDa; theoretical pI, 10.32), both have pI values clearly out of the range resolved by this method. Furthermore, isoelectric focusing of these proteins would require a pH at which methylesters are rapidly hydrolyzed and hence lost from analysis by autoradiography. The inability to detect these PIMT targets highlights the limitations of this method and emphasizes the importance of using complimentary approaches such as acidic reversed phase-high performance liquid chromatography (20) to detect and identify these proteins.

Our real-time linear imaging of PIMT substrates in mouse tissue extracts also only provides a snapshot of proteins that have accumulated isoaspartate, and it does not provide information about isoaspartate stoichiometry or the rates of isoaspartate accumulation. At present we have extrapolated the known properties of proteins to the changes observed in the PIMT KO mouse brain, but further work is required to decipher how increased isoaspartate accumulation specifically alters individual protein functions.

Tissues other than brain taken from *Pcmt1*$^{-/-}$ mice also accumulate PIMT targets, but at much lower quantities than does the brain. We have characterized them herein by molecular weight but they remain to be identified, and their specific tissue abnormalities and contributions to the *Pcmt1*$^{-/-}$ phenotype evaluated. Because no alterations have as yet been discovered in PIMT KO mouse organs other than brain (28) and immune cells (47), the physiological importance of these tissue PIMT targets may be much less than those that induce disruptions of brain protein function. Supporting this is the finding that addition of a neuron-specific PIMT transgene to the *Pcmt1*$^{-/-}$ mice, even though its expression level is low, can relieve the physical and behavioral abnormalities and at least partially restore mouse longevity (28).

With fifteen of the radioactive spots in Fig. 4 remaining to be identified, additional connections between PIMT substrates and the defects present in PIMT KO mice may be observed. These other radioactive spots may represent post-translationally modified forms of the proteins identified herein, previously identified targets, or as yet unidentified PIMT targets. Thus far, however, although PIMT has broad isoaspartate substrate specificity *in vitro*, this study has highlighted that brain cytosolic PIMT activity appears to be primarily focused upon certain proteins: those involved in the regulation of the cytoskeletal architecture, and those involved in vesicular neurotransmitter release.

Acknowledgments—We acknowledge Prof. Dana Aswad (University of California, Irvine), Prof. Mark Mamula and Dr. Hester Doyle (Yale University School of Medicine) for the initial gift of Pcmt1$^{+/+}$ and *Pcmt1*$^{-/-}$ *tissue for pilot assays. We are indebted to Matthew Carlile and John Keyte from the Protein Sequencing Facility (University of Nottingham) for assistance with mass spectrometry. We are grateful to Alexander Rathbone for assistance with proteomics and autoradiographic image analysis. We express our gratitude to the reviewers for their kind and helpful comments for final manuscript preparation.*

REFERENCES

1. Lindner, H., and Helliger, W. (2001) *Exp. Gerontol.* **36,** 1551–1563
2. Clarke, S. (2003) *Ageing Res. Rev.* **2,** 263–285

[3] J. D. Lowenson and S. Clarke, unpublished observation.

3. Reissner, K. J., and Aswad, D. W. (2003) *Cell Mol. Life Sci.* **60,** 1281–1295
4. Robinson, N. E., Robinson, Z. W., Robinson, B. R., Robinson, A. L., Robinson, J. A., Robinson, M. L., and Robinson, A. B. (2004) *J. Pept. Res.* **63,** 426–436
5. Johnson, B. A., Murray, E. D., Clarke, S., Glass, D. B., and Aswad, D. W. (1987) *J. Biol. Chem.* **262,** 5622–5629
6. Johnson, B. A., Langmack, E. L., and Aswad, D. W. (1987) *J. Biol. Chem.* **262,** 12283–12287
7. McFadden, P. N., and Clarke, S. (1987) *Proc. Natl. Acad. Sci. U. S. A.* **84,** 2595–2599
8. Brennan, T. V., Anderson, J. W., Jia, Z. C., Waygood, E. B., and Clarke, S. (1994) *J. Biol. Chem.* **269,** 24586–24595
9. Galletti, P., Ingrosso, D., Manna, C., Clemente, G., and Zappia, V. (1995) *Biochem. J.* **306,** 313–325
10. Ingrosso, D., D'Angelo, S., di Carlo, E., Perna, A. F., Zappia, V., and Galletti, P. (2000) Eur. J. Biochem. **267,** 4397–4405
11. Lanthier, J., and Desrosiers, R. R. (2004) *Exp. Cell Res.* **293,** 96–105
12. Shimizu, T., Matsuoka, Y., and Shirasawa, T. (2005) *Biol. Pharm. Bull.* **28,** 1590–1596
13. Kim, E., Lowenson, J. D., MacLaren, D. C., Clarke, S., and Young, S. G. (1997) *Proc. Natl. Acad. Sci. U. S. A.* **94,** 6132–6137
14. Yamamoto, A., Takagi, H., Kitamura, D., Tatsuoka, H., Nakano, H., Kawano, H., Kuroyanagi, H., Yahagi, Y., Kobayashi, S., Koizumi, K., Sakai, T., Saito, K., Chiba, T., Kawamura, K., Suzuki, K., Watanabe, T., Mori, H., and Shirasawa, T. (1998) *J. Neurosci.* **18,** 2063–2074
15. Shimizu, T., Ikegami, T., Ogawara, M., Suzuki, Y., Takahashi, M., Morio, H., and Shirasawa, T. (2002) *J. Neurosci. Res.* **69,** 341–352
16. Kim, E., Lowenson, J. D., Clarke, S., and Young, S. G. (1999) *J. Biol. Chem.* **274,** 20671–20678
17. Ikegaya, Y., Yamada, M., Fukuda, T., Kuroyanagi, H., Shirasawa, T., and Nishiyama, N. (2001) *Hippocampus* **11,** 287–298
18. Farrar, C., Houser, C. R., and Clarke, S. (2005) *Aging Cell* **4,** 1–12
19. Farrar, C. E., Huang, C. S., Clarke, S. G., and Houser, C. R. (2005) *J. Comp. Neurol.* **493,** 524–537
20. Young, A. L., Carter, W. G., Doyle, H. A., Mamula, M. J., and Aswad, D. W. (2001) *J. Biol. Chem.* **276,** 37161–37165
21. Reissner, K. J., Paranandi, M. V., Luc, T. M., Doyle, H. A., Mamula, M. J., Lowenson, J. D., and Aswad, D. W. (2006) *J. Biol. Chem.* **281,** 8389–8398
22. O'Connor, M. B., and O'Connor, C. M. (1998) *J. Biol. Chem.* **273,** 12909–12913
23. Ohta, K., Seo, N., Yoshida, T., Hiraga, K., and Tuboi, S. (1987) *Biochimie* (*Paris*) **69,** 1227–1234
24. Najbauer, J., Orpiszewski, J., and Aswad, D. W. (1996) *Biochemistry* **35,** 5183–5190
25. Lanthier, J., Bouthillier, A., Lapointe, M., Demeule, M., Beliveau, R., and Desrosiers, R. R. (2002) *J. Neurochem.* **83,** 581–591
26. Aswad, D. W., and Deight, E. A. (1983) *J. Neurochem.* **40,** 1718–1726
27. MacLaren, D. C., and Clarke, S. (1995) *Protein Expr. Purif.* **6,** 99–108
28. Lowenson, J. D., Kim, E., Young, S. G., and Clarke, S. (2001) *J. Biol. Chem.* **276,** 20695–20702
29. Lees, J. E., and Richards, P. G. (1999) *Electrophoresis* **20,** 2139–2143
30. Laemmli, U. K. (1970) *Nature* **227,** 680–685
31. Freitag, C., and Clarke, S. (1981) *J. Biol. Chem.* **256,** 6102–6108
32. Richards, P., and Lees, J. (2002) *Proteomics* **2,** 256–261
33. Richards, P. G., Johnson, M. K., and Ray, D. E. (2000) *Mol. Pharmacol.* **58,** 577–583
34. Mizobuchi, M., Murao, K., Takeda, R., and Kakimoto, Y. (1994) *J. Neurochem.* **62,** 322–328
35. Teshima, G., Hancock, W. S., and Canova-Davis, E. (1995) in *Deamidation and Isoaspartate Formation in Peptides and Proteins* (Aswad, D. W., ed) pp. 167–192, CRC Press, Inc., Boca Raton, FL
36. Murphy, D. D., Rueter, S. M., Trojanowski, J. Q., and Lee, V. M. Y. (2000) *J. Neurosci.* **20,** 3214–3220
37. Totterdell, S., Hanger, D., and Meredith, G. E. (2004) *Brain Res.* **1004,** 61–72
38. Cabin, D. E., Shimazu, K., Murphy, D., Cole, N. B., Gottschalk, W., McIlwain, K. L., Orrison, B., Chen, A., Ellis, C. E., Paylor, R., Lu, B., and Nussbaum, R. L. (2002) *J. Neurosci.* **22,** 8797–8807
39. Liu, S. M., Ninan, I., Antonova, I., Battaglia, F., Trinchese, F., Narasanna, A., Kolodilov, N., Dauer, W., Hawkins, R. D., and Arancio, O. (2004) *EMBO J.* **23,** 4506–4516
40. George, J. M., Jin, H., Woods, W. S., and Clayton, D. F. (1995) *Neuron* **15,** 361–372
41. Shibayama-Imazu, T., Okahashi, I., Omata, K., Nakajo, S., Ochiai, H., Nakai, Y., Hama, T., Nakamura, Y., and Nakaya, K. (1993) *Brain Res.* **622,** 17–25
42. Chandra, S., Fornai, F., Kwon, H. B., Yazdani, U., Atasoy, D., Liu, X. R., Hammer, R. E., Battaglia, G., German, D. C., Castillo, P. E., and Sudhof, T. C. (2004) *Proc. Natl. Acad. Sci. U. S. A.* **101,** 14966–14971
43. Layfield, R., Lowe, J., and Bedford, L. (2005) *Essays Biochem.* **41,** 157–171
44. Yeung, K., Seitz, T., Li, S. F., Janosch, P., McFerran, B., Kaiser, C., Fee, F., Katsanakis, K. D., Rose, D. W., Mischak, H., Sedivy, J. M., and Kolch, W. (1999) *Nature* **401,** 173–177
45. Trakul, N., Menard, R. E., Schade, G. R., Qian, Z. H., and Rosner, M. R. (2005) *J. Biol. Chem.* **280,** 24931–24940
46. Frayne, J., Ingram, C., Love, S., and Hall, L. (1999) *Cell Tissue Res.* **298,** 415–423
47. Doyle, H. A., Gee, R. J., and Mamula, M. J. (2003) *J. Immunol.* **171,** 2840–2847
48. Ojika, K., Mitake, S., Tohdoh, N., Appel, S. H., Otsuka, Y., Katada, E., and Matsukawa, N. (2000) *Prog. Neurobiol.* **60,** 37–83
49. Johnson, G. V. W., and Jope, R. S. (1992) *J. Neurosci. Res.* **33,** 505–512
50. Lewis, S. A., Ivanov, I. E., Lee, G. H., and Cowan, N. J. (1989) *Nature* **342,** 498–505
51. Bernhardt, R., and Matus, A. (1984) *J. Comp. Neurol.* **226,** 203–221
52. Belmont, L. D., and Mitchison, T. J. (1996) *Cell* **84,** 623–631
53. Ravelli, R. B. G., Gigant, B., Curmi, P. A., Jourdain, I., Lachkar, S., Sobel, A., and Knossow, M. (2004) *Nature* **428,** 198–202
54. Di Paolo, G., Pellier, V., Catsicas, M., Antonsson, B., Catsicas, S., and Grenningloh, G. (1996) *J. Cell Biol.* **133,** 1383–1390
55. Iancu-Rubin, C., and Atweh, G. F. (2005) *Trends Cell Biol.* **15,** 346–348
56. Rappoport, J. Z., Taha, B. W., and Simon, S. M. (2003) *Traffic* **4,** 460–467
57. Goud, B., Huet, C., and Louvard, D. (1985) *J. Cell Biol.* **100,** 521–527
58. Jockusch, W. J., Praefcke, G. J. K., McMahon, H. T., and Lagnado, L. (2005) *Neuron* **46,** 869–878
59. Kittler, J. T., Delmas, P., Jovanovic, J. N., Brown, D. A., Smart, T. G., and Moss, S. J. (2000) *J. Neurosci.* **20,** 7972–7977
60. Williams, D. B. (2006) *J. Cell Sci.* **119,** 615–623
61. Bedard, K., Szabo, E., Michalak, M., and Opas, M. (2005) *Int. Rev. Cytol.* **245,** 91–121
62. Potter, S. M., Johnson, B. A., Henschen, A., Aswad, D. W., and Guzzetta, A. W. (1992) *Biochemistry* **31,** 6339–6347
63. Hilfiker, S., Pieribone, V. A., Czernik, A. J., Kao, H. T., Augustine, G. J., and Greengard, P. (1999) *Philos. Trans. R. Soc. Lond B. Biol. Sci.* **354,** 269–279
64. Schwartz, R., Ting, C. S., and King, J. (2001) *Genome Res.* **11,** 703–709